NASA-TM-100591
19880014372

NASA Technical Memorandum 100591

UNSTEADY PRESSURE AND STRUCTURAL RESPONSE MEASUREMENTS OF AN ELASTIC SUPERCRITICAL WING

Clinton V. Eckstrom, David A. Seidel, and Maynard C. Sandford

MAY 1988

National Aeronautics and
Space Administration

Langley Research Center
Hampton, Virginia 23665

UNSTEADY PRESSURE AND STRUCTURAL RESPONSE MEASUREMENTS ON AN ELASTIC SUPERCRITICAL WING

Clinton V. Eckstrom, David A. Seidel, and Maynard C. Sandford

NASA Langley Research Center
Hampton, Virginia 23665-5225

Abstract

Results are presented which define unsteady flow conditions associated with high dynamic response experienced on a high aspect ratio elastic supercritical wing at transonic test conditions while being tested in the NASA Langley Transonic Dynamics Tunnel. The supercritical wing, designed for a cruise Mach number of 0.80, experienced the high dynamic response in the Mach number range from 0.90 to 0.94 with the maximum response occurring at a Mach number of approximately 0.92. At the maximum wing response condition the forcing function appears to be the oscillatory chordwise movement of strong shocks located on both the wing upper and lower surfaces in conjunction with the flow separating and reattaching in the trailing edge region.

Nomenclature

C_p	pressure coefficient
C_p^*	critical pressure coefficient, two dimensional value
G	acceleration / gravitational constant
Hz	Hertz, cycles/second
M	free stream Mach number
q	free stream dynamic pressure, psf
SGB	output of wing root strain gage bridge
x/c	fraction of local chord
η	fraction of semispan

Introduction

The elastic supercritical wing used in the present test is the full-scale right semispan of the second Aeroelastic Research Wing (ARW-2). This research wing was designed to be flown on a drone flight aircraft for the investigation of active control systems for maneuver load alleviation, gust load alleviation, and flutter suppression (reference 1). The flight wing structural design was based on an iterative procedure which took into account the load and stiffness reduction benefits provided by the active control systems. This integrated design process resulted in a wing with more flexibility than otherwise would have occurred. A delay in the planned drone flight-test program provided the opportunity to use the instrumented flight wing as a flexible model for testing in the Langley Transonic Dynamics Tunnel (TDT) as part of a continuing series of tests for measurement of unsteady transonic aerodynamic characteristics on various wing planforms and airfoil shapes (reference 2). In preparation for flight tests of the flexible wing there were wind-tunnel tests of a structurally stiff 0.237-scale model of the flight wing and drone fuselage (references 3 and 4). These scale-model tests identified that the drag-divergence Mach number for this supercritical wing configuration occurs in the Mach number range 0.81 to 0.83. Drag-divergence is an indicator of the onset of the breakdown in attached flow conditions.

During the initial wind-tunnel test of this elastic wing (reference 5) a region of high dynamic response characterized by wing first bending motion was unexpectedly encountered near M=0.90. Analysis of wing response data using a subcritical response technique appeared to predict an instability boundary at an almost constant Mach number of 0.90 for all test dynamic pressures. Consequently, further testing was limited to M=0.88 or less to prevent possible damage to the wing which was still considered to be a flight article. Although a change in flow characteristics at Mach numbers higher than drag-divergence was expected, the occurrence of large amplitude wing response motion, and the resulting prediction of an instability boundary, were not anticipated.

As a result of continued interest in the large amplitude wing response experienced during the first tunnel test and the subsequent cancellation of the flight-test program, a second tunnel test was conducted without a Mach number limitation to specifically investigate the region of large wing response. No instability boundary was found during the second test, but rather a narrow Mach number region through which the wing experiences high dynamic response (reference 6). The response, which increased in magnitude as the test dynamic pressure was increased, is centered near a Mach number of 0.92.

The goal for the second tunnel test was not only to fully explore the region of large wing response and determine if an instability boundary existed but also to define the unsteady flow conditions forcing the response. The flexible ARW-2 wing was instrumented for the measurement of unsteady pressures on the outboard portion of the right semispan in preparation for the drone flight-test program. Measurement requirements for the first wind-tunnel test resulted in the data being recorded for discrete test points to provide mean pressure values for static test conditions and transfer function magnitude and phase information for con-

trol surface oscillation tests. In order to provide better information on wing surface flow conditions the data acquisition procedure was modified for the second test so that continuous wing surface pressure time history measurements were recorded. A summary of initial results from the second tunnel test were reported in reference 6. The conclusion that the driving mechanism appears to be related to chordwise shock movement in conjunction with flow separation and reattachment on both the wing upper and lower surfaces resulted from evaluation of the measured surface pressure time histories.

This paper presents sample results from an ongoing evaluation of the measured wing motions and wing surface-pressure time histories. Chordwise pressure distributions as well as pressure time histories are presented to show the degree of flow unsteadiness through the transonic speed range where the high dynamic response was encountered. The effects of changes in test dynamic pressure and model angle of attack on mean value pressure distributions are also presented.

Model

The right semispan of the full-scale wing used as the test model is shown mounted on the TDT test-section sidewall in figure 1. The supercritical wing model has a semispan length of 9.5 ft., an aspect ratio of 10.3, and a leading edge sweep angle of 28.8 degrees. The half-body fuselage has ojive nose and tail sections but is of cylindrical shape with a diameter of 25 inches in the region of the wing mounting. Wing planform and dimensional data are presented in figure 2. The wing frequency response characteristics measured in still air are shown in figure 3. The four nodal frequencies noted in figure 3 are for the wing first bending, wing second bending, fore and aft in plane, and wing first torsion modes, respectively.

Instrumentation

Locations for the wing surface-pressure orifices and the accelerometers are presented in the planform layout of figure 2. The wing surface pressures were measured using a separate electronically scanned pressure (ESP) measurement system (reference 7) for each orifice row. Each ESP module contained 32 pressure transducers all of which had a common reference pressure port. For this test setup the reference pressure was the tunnel static pressure. The wing surface orifices were connected to the pressure transducers by matched metal and plastic tubes having an inner diameter of 0.040 inch and a length of 18 inches. There were 16 orifices on both the upper and lower surfaces of the inboard orifice row and 15 orifices each on the upper and lower surfaces of the other five orifice rows for a total of 182 wing surface pressure measurements. An additional eight in-situ pressure transducers were located side by side with some of the fifth row orifices for calibration purposes.

Wing vertical response motion was measured using ten accelerometers located along the wing front and rear spars with the distribution shown in figure 2. Although not shown in figure 2 the wing was also equipped with several strain-gage bridges calibrated for the measurement of shear, bending moment, and torsion loads (reference 8).

Data Acquisition

Data from the three inboard rows of orifices were acquired at a rate of 31.25 samples per second while for the three outboard rows of orifices the data were acquired at a rate of 250 samples per second. Data from the outboard six accelerometers and for four strain-gage bridges were also taken at a rate of 250 samples per second. The four strain-gage bridges used were located two each on the front and rear spars near the wing root. Data from the three outboard orifice rows, the wing tip leading edge accelerometer, and the wing root rear spar bending moment strain-gage bridge were used for the analysis results presented herein.

Wind Tunnel

The model was tested in the Langley Research Center Transonic Dynamics Tunnel (TDT) which is a closed circuit continuous-flow tunnel with a 16-foot square test section with slots in all four walls. Mach number and dynamic pressure can be varied simultaneously, or independently, with either air or Freon as the test medium. Freon was used for the testing reported herein.

Test Results and Discussion

The supercritical wing model was tested by making runs at three different dynamic pressure (q) levels as a function of Mach number as shown by the data in figure 4. The tunnel was operated by setting a total pressure and then increasing the motor fan speed until the desired test condition was reached. As a result the test dynamic pressure increased slightly with Mach number during each run as shown in the figure. The dynamic pressure at M=0.92 for the low q, medium q, and high q test conditions were 78 psf, 152 psf, and 318 psf, respectively. Also shown in figure 4 is the region where high dynamic wing motion response was observed and measured as well as the predicted linear theory flutter boundary which is located at a much higher dynamic pressure level than where the wing was tested.

At the low q test conditions all data were acquired at an angle of attack of zero degrees. For the medium q test conditions the angle of attack was varied from -2 to +2

degrees in one degree increments. For the high q test condition the primary angle of attack was zero degrees although a few test points were obtained at +/- 1 degree angle of attack. Unless otherwise stated the data presented are for an angle of attack of zero degrees.

Wing Response Measurements

Accelerometer measurement time histories and results from real time response analysis of the accelerometer signals are presented in figure 5 for the high q test condition to illustrate the rapid growth and then the equally rapid decay of wing response as Mach number was increased from 0.80 up to 0.96. The test Mach numbers selected are representative of conditions before any significant wing motion occurred (M=0.80), during buildup of wing motion (M=0.88), near maximum wing response (M=0.92), and after wing motion had subsided (M=0.96). The response measurements show that the frequencies for the large wing responses were in the 8 to 10 Hz range, which indicates that wing first bending mode type motion was occurring.

During post test analysis, a 10.24 second record of data was analyzed to define a power spectral density (PSD) curve for each of the test conditions shown previously in figure 4. For each test condition the maximum accelerometer PSD value in the 8 to 10 Hz frequency range was established. These maximum or peak PSD values are presented in figure 6 as a function of Mach number for each of the three dynamic pressure test conditions to show the narrow Mach number range through which the wing experienced the high dynamic response. The results presented in figure 6 also show that the peak values increased in magnitude as the test dynamic pressure increased and that the maximum wing response occurred near M=0.92 for all three dynamic pressure test conditions.

Presentation of Surface Pressure Measurements

Wing surface-pressure measurements are most often presented as chordwise distributions of time averaged or mean values of pressure coefficients for specific test conditions. Mean value results may be used because of instrumentation limitations which preclude getting valid time history measurements, or mean value pressures may be used simply as a way to present a large number of results in a compact and efficient manner. Unfortunately, such a presentation method can mask time varying or unsteady flow conditions that can be identified by looking at pressure measurement time histories. To illustrate this point, figure 7 presents both chordwise distributions of pressure coefficient mean values and samples of pressure coefficient time history measurements from four typical orifice locations on the wing upper and lower surfaces as shown on the airfoil schematic. The C_p^* value shown on the chordwise pressure distributions is the pressure coefficient at which the flow would reach sonic velocity on a model as determined for two dimensional flow conditions. It is an approximate value for the three dimensional flow conditions of this test series. However, it is a good indicator that supersonic flow conditions exist when the pressure coefficient increases above this value. The measurements are for wing semispan station $\eta = .87$ (fifth row of pressure orifices). Data are presented for the four Mach numbers which span the transonic speed range of interest. The results are for the high q test conditions for which wing-response accelerometer measurements were presented previously in figure 5.

At M=0.80 the chordwise distribution shows that the pressure coefficient mean values are near the C_p^* value for the forward portion of the chord. The time histories of pressure coefficient for this test condition show some flow unsteadiness at all locations but with the largest response at location 1. No coherent low frequency content is noticeable in the pressure measurements nor was any significant wing motion observed. At M=0.88 the chordwise pressure distribution shows that the flow is supersonic over the forward portion of the chord. From the sample time histories of pressure coefficients we can get an idea of just how unstable the flow is for this test condition. At location 1, which is just ahead of the strong shock on the upper surface, the flow is quite smooth. However, the situation is substantially different for locations 2, 3, and 4 where very large variations in pressure coefficients are occurring. Although the measured pressure variations at the M=0.88 test condition are large the wing motion was considered moderate and not of sufficient magnitude to cause concern. For the M=0.92 test condition the chordwise distribution of pressure coefficient mean values indicates that a strong shock has developed on both the wing upper and lower surfaces. The flow is quite smooth at locations 1 and 3 which are ahead of the shocks but very unsteady at locations 2 and 4 which are in the region of the shocks. The M=0.92 test condition is where the large amplitude wing motions of concern were experienced. At M=0.96 the chordwise pressure distribution indicates the flow is supersonic over the entire chord and the time histories indicate smooth flow at each of the four sample orifice locations. Wing motion at the M=0.96 test condition was insignificant.

The mean value chordwise pressure distributions of figure 7 also give information on when trailing edge flow separation occurs. For this supercritical airfoil the upper surface pressure coefficient curve should cross from above to below the zero line near x/c = .95 for attached flow conditions. Separated flow conditions are definitely indicated if the upper surface trailing edge pressure measurement at x/c = .99 approaches or crosses to the upper side of the zero line. Using this criteria the mean-value pressure coefficients indicate that the upper surface trailing edge flow is attached at M=0.80 and 0.88, a slight change is observed for M=0.92, and the flow has definitely separated at M=0.96. For the wing lower surface, attached flow through the trailing edge cove region of the supercritical airfoil produces

the trailing edge pressure coefficient profile shown for the M=0.80 and 0.88 test conditions. When the flow on the lower surface separates the pressure coefficients for the cove region move up toward the zero line. Using this criteria the mean-value pressure coefficients indicate that the lower surface trailing edge flow has separated for the M=0.92 test condition. For the M=0.96 test condition the region of flow separation on the lower surface trailing edge increased further causing the pressure coefficients to go above the zero line as shown. Wool tufts mounted on the wing surfaces (reference 6) were used to give a visual confirmation of when flow separation occurred.

Chordwise Pressure Distributions

From the data of figure 7 it is obvious that it is useful to look at both the mean value of the pressure coefficients and to have an idea of the magnitude of the pressure variation that is occurring at each measurement location. Chordwise pressure distributions showing the pressure coefficient measurement range at each orifice location as well as the mean values are presented in figure 8 for spanwise station η = .87 for the same four high q test conditions shown previously in figures 5 and 7. The pressure coefficient measurement range is shown in the form of a vertical bar which goes from the maximum to the minimum value measured at each orifice location. The mean values and the range between minimum and maximum values were determined for a four-second time interval for each test condition. Range was selected as the method to show the pressure variations because of the nonperiodic form of the measurements at several locations. The upper surface and lower surface pressure measurements are shown separately in order to prevent overlapping of data.

The data presented in figure 8 show that even at M=0.80 there is a large region of unsteady flow on the wing upper surface (x/c = 0.29 to 0.58). Because M=0.80 was the design cruise Mach number for the flight wing this region of flow unsteadiness was not expected although it did not seem to cause any significant wing response motion as was discussed earlier. At M=0.88 the upper surface measurement ranges are largest at and near the shock location. For the wing lower surface the range of measured pressure variations is quite large in the midchord region (x/c = 0.30 to 0.51) which may represent shock movement over a large chordlength. Both the trailing edge pressure coefficient measurements and the wool tufts indicated that the flow remained attached in the outboard region of the wing for this test condition. Although the pressure measurement ranges are very large at M=0.88 the wing experienced only moderate response motion at this test condition as was mentioned earlier.

The pressure distributions of figure 8 for M=0.92 show a large region of stable supersonic flow followed by a strong shock on both the wing upper and lower surfaces. The largest measurement ranges occur at the shock locations with smaller, but still significant, measurement ranges occurring in the trailing edge region behind the shocks, particularly for the wing lower surface. The pressure-measurement range at the wing upper surface trailing edge location indicates that the flow is alternating between attached and detached flow conditions. On the lower surface from x/c = .68 to the trailing edge the ranges for the pressure measurements indicate that there is alternating separated and attached flow throughout the lower surface cove region. The wool tufts (reference 6) indicated separated flow from x/c = 0.7 to 1.0 on the wing upper surface and from 0.6 to 1.0 on the lower surface for the entire outboard wing region. The M=0.92 test condition is where the largest amplitude wing response motions occurred. At M=0.96, where wing motion is very small, the flow is supersonic over the entire chord on both the wing upper and lower surfaces. Even so there still seems to be a strong shock at x/c = .74 on the upper surface and between x/c = .74 and .83 on the lower surface. The only large measurement range observed occurs on the wing upper surface at the strong shock location. The wool tufts (reference 6) indicated separated flow from x/c = 0.6 to 1.0 for both the upper and lower surfaces.

The chordwise pressure distribution presentation format of figure 8 does provide a good understanding of the overall flow condition at the wing station and an idea of the location and magnitude of local pressure variations. However, it does not provide information on frequency content, phasing, or coherency of any of the pressure oscillations that are occurring. A better understanding of the oscillatory characteristics of each measurement can be obtained by looking directly at the surface pressure measurement time histories as presented in the next section.

Surface Pressure Measurement Time Histories

Examples of wing surface pressure coefficient measurement time histories are presented in figures 9 and 10 for the Mach number 0.88 and 0.92 high q test conditions, respectively. These are the test conditions where large ranges in measured pressures were observed for chordwise pressure distribution results at semispan station η = .87 (fig. 8). The three columns of time-history measurements in figures 9 and 10 are for all three outboard orifice rows where high sample rate measurements were obtained. As indicated on the figures, the upper 15 pressure measurements in each column are from the wing upper surface and the lower 15 from the wing lower surface. The zero pressure coefficient locations and the x/c positions are provided for each pressure trace as well as a scale applicable to all of the pressure coefficient measurements. No pressure measurements are given for the first three orifice locations on the lower surface at the inboard station because they were found to be invalid. The purpose of presenting measurements from all three outboard orifice rows is to show that there are also some significant spanwise variations in unsteady pressures at each

test condition. The output of the wing root rear spar bending moment strain-gage bridge (SGB) is presented at the bottom of each column of pressure measurements to show the relationship between local pressure oscillations and wing motion. For wing first bending mode motion, wing root bending moment is proportional to wing deflection.

Chordwise distributions of pressure coefficent mean values are presented in figure 11 for the same orifice rows and test conditions as the time-history measurements of figures 9 and 10. Correlation of pressure coefficent time-history measurements of figures 9 and 10 with the mean value chordwise distributions of figure 11 assists in visualizing shock locations and other flow conditions influencing vertical spacing of the time-history measurements.

The pressure coefficient time histories presented in figure 9 for M=0.88 show that large amplitude pressure variations are occurring at several locations on each orifice row. A predominate feature for the wing upper surface is the large vertical spacing between measurements associated with strong shock locations. At η = .71 the large vertical spacing between measurements at x/c = .66 and .74 results from the large negative pressure gradient associated with the strong shock situated between these two measurement locations. The large vertical spikes in the measurement at x/c = .74 occur when the shock moves across and aft of that measurement location. A noticeable spanwise variation is that the shock location moves progressively further forward for the middle and outboard orifice rows. On the wing lower surface there is a large pressure gradient at the outboard orifice row (η = .97) between x/c = .29 and .36 indicating the existence of a strong shock. However, at the two more inboard stations (η = .71 and .87) the existence of a strong shock is not as obvious. Rather, it appears that a large pressure wave is oscillating back and forth across several orifice locations (x/c = .30 to .57 for η = .87). Even though there are many orifice locations where large amplitude pressure oscillations are occurring the wing motion as shown by the SGB output was very moderate.

The predominate feature of the pressure time histories presented in figure 10 for M=0.92 are the large amplitude pressure oscillations associated with the strong shocks on both the wing upper and lower surfaces at all three semispan stations. Pressure oscillations at other x/c locations appear to increase in amplitude from the inboard to the outboard station. The SGB measurement shows the wing motion for comparison with wing surface pressure oscillations. As stated previously the response motion for this test condition was very large resulting in concern for the structural safety of the wing.

A few observations can be made concerning the time-history measurements of figure 10. Because the SGB measurement is proportional to wing deflection the downward slope of the SGB trace corresponds to plunge motion resulting in an increase in local angle of attack. Conversely, the upward slope of SGB corresponds to heave motion and a decrease in local angle of attack. The largest wing-deflection motion and, therefore, the largest effect of local angle of attack changes would be at the wing-tip station (η = .97) for first bending motion. Furthermore, the largest effects due to angle of attack changes would be expected in the wing leading edge region. As can be seen, the wing leading edge pressure time-history oscillations are largest for the wing outboard station and they do correlate with the wing motion. For the wing upper surface leading edge (x/c = .02 to .23) the increased amplitude portion of the pressure oscillation correlates with plunge motion or increased angle of attack. Conversely, for the lower surface (x/c = .02 to .36) the increased amplitude portion of the pressure oscillation correlates with heave motion or a decrease in local angle of attack. Further, it is observed that the pressure oscillation associated with shock movement on the wing upper surface (x/c = .56) is out of phase with the pressure oscillations in the wing leading edge area indicating that the shock moves forward with increasing angle of attack (plunge) and aft with decreasing angle of attack (heave). The pressure oscillations associated with the strong shocks on the lower surface at each semispan do not correlate well with the other pressure oscillations. However, the pressure oscillations aft of the shocks on both the wing upper and lower surfaces are coherent but do show varying phase shifts. Determination of the significance of the pressure oscillations and their combined effect in forcing wing response is the major remaining task in the evaluation process.

Cp Variations With Test Dynamic Pressure

The effects of changes in test dynamic pressure on the chordwise distribution of pressure coefficient mean values are presented in figure 12 for spanwise station η = .87 for Mach numbers 0.85 and 0.92. The pressure coefficient mean value is the calculated average of the measurements at each orifice location for a four second data interval. The Mach number selected for presentation of data prior to maximum wing response was changed from M=0.88 to M=0.85 because data was not available for the low q test condition at M=0.88.

At M=0.85 the mean value pressure coefficients for the forward portion of the chord indicate that the airfoil section is effectively twisting downward to a more negative angle of attack as the dynamic pressure is increased. This is consistent with washout due to bending for an aft swept wing subjected to increased loading. At M=0.92 the largest differences in mean value pressure coefficient chordwise distributions for the upper surface are at the strong shock location and in the trailing edge region. The data do not show a consistent trend since the upper surface shock is farthest aft for the medium q test condition. On the lower surface at M=0.92 the small changes in mean value pressure coefficients for the forward portion of the chord are consistent with

decreasing local angle of attack with increasing test dynamic pressure. More significant differences occur on the aft portion of the chordline where the negative pressure gradient is much steeper for the two higher q test conditions and at the high q test condition the upward movement of the pressure coefficients in the trailing edge region indicate that significant flow separation has occurred.

Cp Variations with Angle of Attack

The effects of changes in angle of attack on the chordwise distribution of pressure coefficient mean values are presented in figure 13 for spanwise station $\eta = .87$ for the medium q test condition for Mach numbers 0.85 and 0.92. For both Mach numbers the mean value pressure coefficients on the forward portion of the chord increase with angle of attack on the upper surface and decrease with angle of attack on the lower surface as would be expected.

At M=0.85 the mean value pressure distributions show the existence of a strong shock on the upper surface for the two higher angles of attack. Also at M=0.85 the mean value pressure coefficients on the aft portion of the chord are essentially independent of angle of attack as is normal for the supercritical airfoil shape. However, at M=0.92 there are some angle of attack effects on the wing lower surface mean value pressure distribution at the aft portion of the chord for

At M=0.85 the mean-value pressure distributions show the existence of a strong shock on the upper surface for the two higher angles of attack. Also at M=0.85 the mean value pressure coefficients on the aft portion of the chord are essentially independent of angle of attack as is normal for the supercritical airfoil shape. However, at M=0.92 there are some angle of attack effects on the wing lower surface mean-value pressure distribution at the aft portion of the chord for the two most negative angles. It is believed that the changes result from more extensive flow separation at the lower surface trailing edge region for the more negative angles of attack.

Concluding Remarks

The high-aspect ratio flexible supercritical wing was tested in the Langley Transonic Dynamics Tunnel to investigate a region of large wing response that occurred in the transonic speed range. Accelerometer measurements indicated that significant wing-tip motions occurred between test Mach numbers of 0.90 and 0.94 with the peak response occurring at about M=0.92. Variation of test dynamic pressure revealed that the Mach number region of high response remained the same and that the magnitude of wing-tip motion increased as the test dynamic pressure was increased. At the peak-response test condition the wing motion was of sufficient magnitude to cause concern for the structural safety of the wing.

Continuous wing surface pressure time-history measurements were obtained as part of an effort to define the unsteady flow conditions forcing the response motion. The time-history measurements revealed that some unsteady flow existed even at the wing design cruise Mach number of 0.80 although no significant wing motion occurred. As the Mach number was increased to 0.88, the wing upper surface developed steady supersonic flow over the forward chord followed by a strong shock whose location oscillated back and forth across at least one orifice location. Pressure measurements on the wing lower surface at M=0.88 revealed large variations at several midchord measurement locations at each span station. Although the measured pressure variations were very large at M=0.88 the wing experienced only moderate response motion at this test condition. As the Mach number was increased to 0.92, the wing developed supersonic flow over the forward portion of the chord followed by strong shocks on both the wing upper and lower surfaces. The largest amplitude pressure variations occurred at the strong shock locations with smaller variations primarily aft of the shock in the trailing edge region where flow separation was occurring, particularly on the wing lower surface. As stated previously, the wing motion at this test condition was of sufficient magnitude to cause concern for wing structural safety. When the test Mach number was increased to M=0.96, the pressure measurements exhibited very small dynamic variations and the wing motion essentially disappeared.

Steady and unsteady flow conditions have been defined for the test conditions where maximum wing dynamic response occurred. The forcing function appears to be the oscillatory chordwise movement of strong shocks located on both the wing upper and lower surfaces in conjunction with the flow separating and reattaching in the trailing edge region. Several significant spanwise variations in steady and unsteady pressures were noted. Future efforts will be directed toward defining the phase relationships between the unsteady pressures, the integrated pressure forces, and the wing motion.

References

1. Murrow, H. N.; and Eckstrom, C. V.: Drones for Aerodynamic and Structural Testing (DAST) - A Status Report. Journal of Aircraft, Vol. 16, No. 8, August 1979, pp. 521-526.

2. Sandford, M. C.; Ricketts, R. H.; and Hess, R. W.: Recent Transonic Unsteady Pressure Measurements at the NASA Langley Research Center. NASA TM-86408, April 1985.

3. Byrdsong, T. A.; and Brooks, C. W., Jr.: Wind-Tunnel Investigation of Longitudinal and Lateral-Directional Stability and Control Characteristics of a 0.237-Scale Model of

a Remotely Piloted Research Vehicle With a Thick, High-Aspect-Ratio Supercritical Wing. NASA TM-81790, July 1980.

4. Byrdsong, T. A.; and Brooks, C. W., Jr.: Wind-Tunnel Investigation of Aerodynamic Loading on a 0.237-Scale Model of a Remotely Piloted Vehicle With a Thick, High-Aspect-Ratio Supercritical Wing. NASA TM-84614, June 1983.

5. Seidel, D. A.; Sandford, M. C.; and Eckstrom, C. V.: Measured Unsteady Transonic Aerodynamic Characteristics of an Elastic Supercritical Wing. Journal of Aircraft, Vol. 24, No. 4, April 1987, p. 225.

6. Seidel, D. A.; Eckstrom, C. V.; and Sandford, M. C.: Investigation of Transonic Region of High Dynamic Response Encountered on an Elastic Supercritical Wing. AIAA Paper No. 87-0735-CP, April 1987.

7. Chapin, W. G.: Dynamic-Pressure Measurements Using an Electronically Scanned Pressure Module. NASA TM 84650, July 1983.

8. Eckstrom, C. V.: Loads Calibration of Strain Gage Bridges on the DAST Project Aeroelastic Research Wing (ARW-2). NASA TM 87677, March 1986.

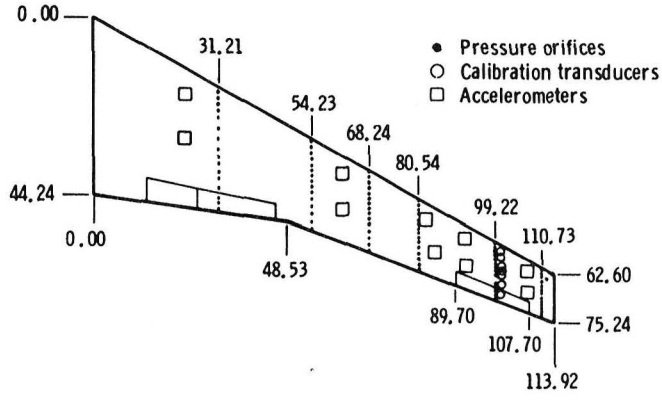

Figure 2.- Wing planform and instrumentation locations (in inches).

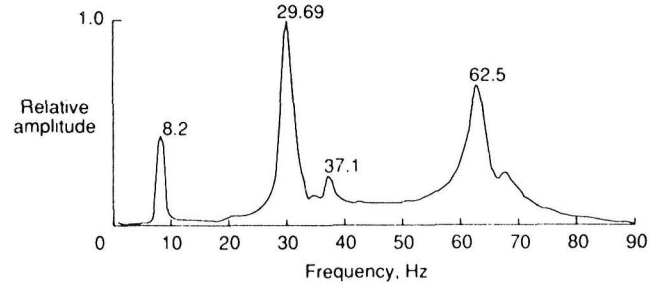

Figure 3.- Wing frequency response characteristics measured in still air.

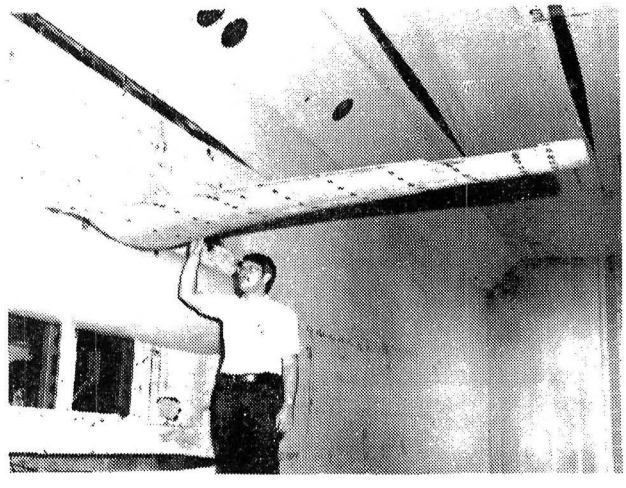

Figure 1.- Wing mounted in TDT test section.

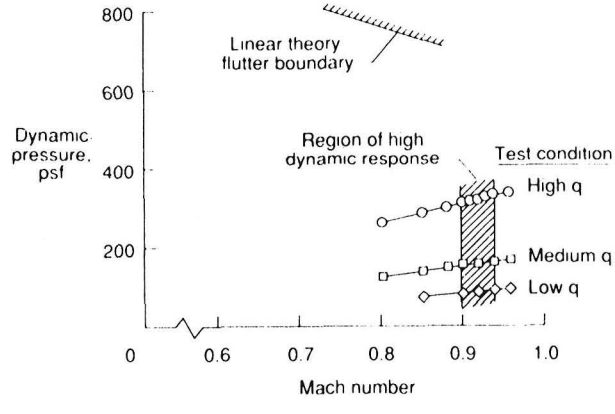

Figure 4.- Test conditions.

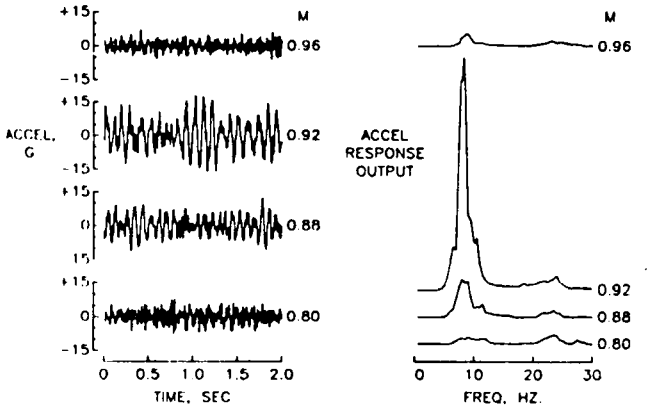

a) Time history data. b) Frequency analysis results.

Figure 5.- Wing response measurements for high q test condition.

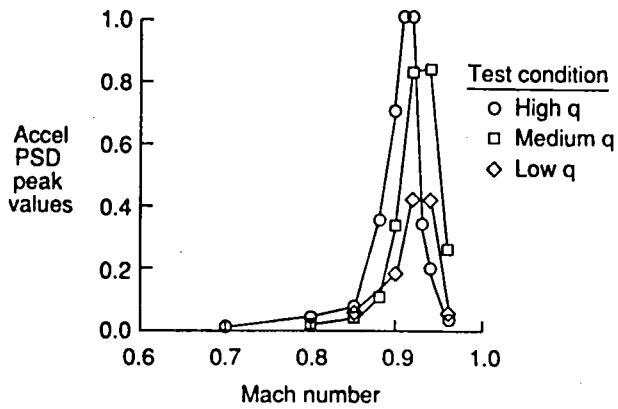

Figure 6.- Accelerometer PSD peak responses.

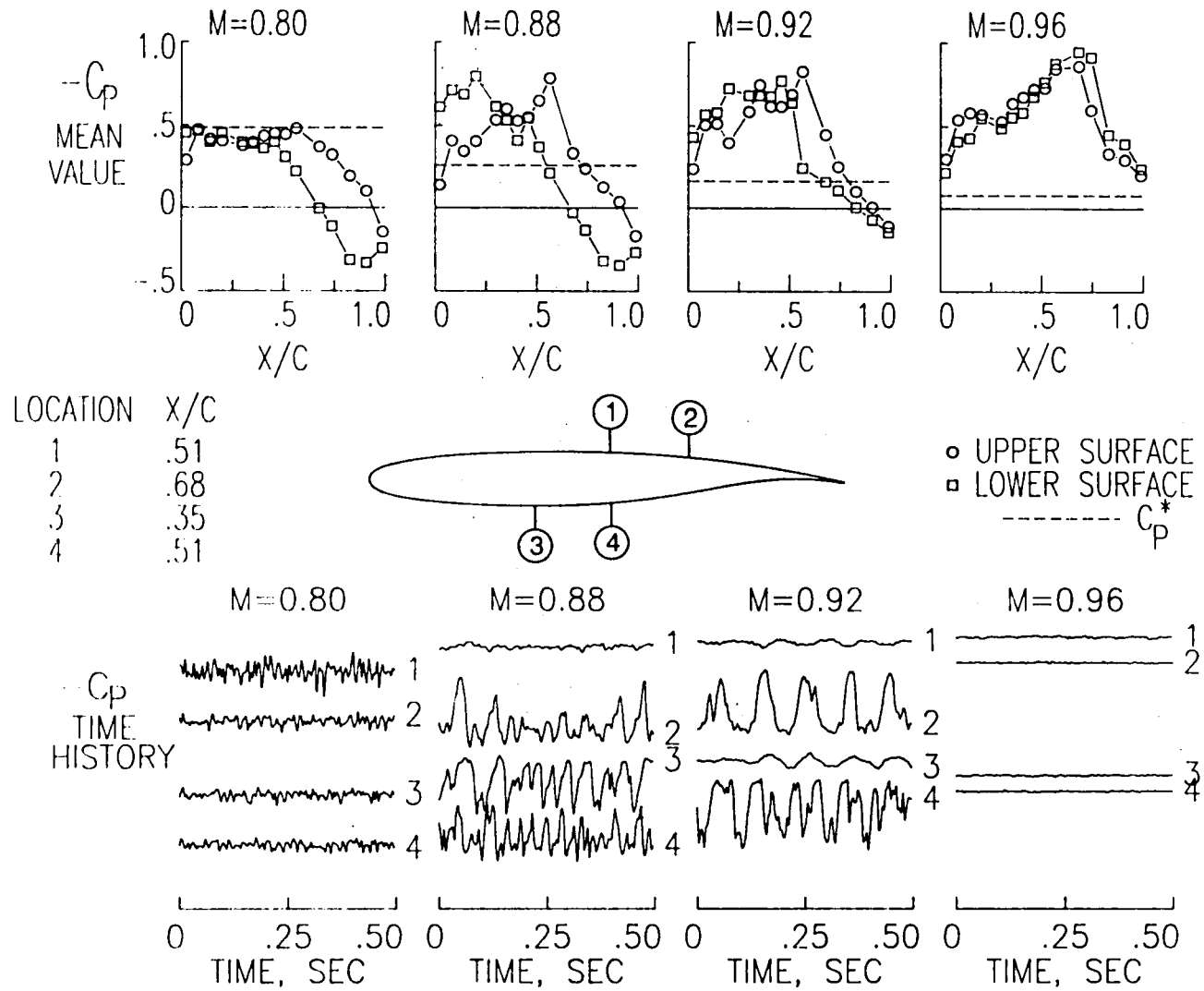

Figure 7.- Mean value chordwise pressure distributions and sample pressure measurement time histories (high q test condition, η=.87).

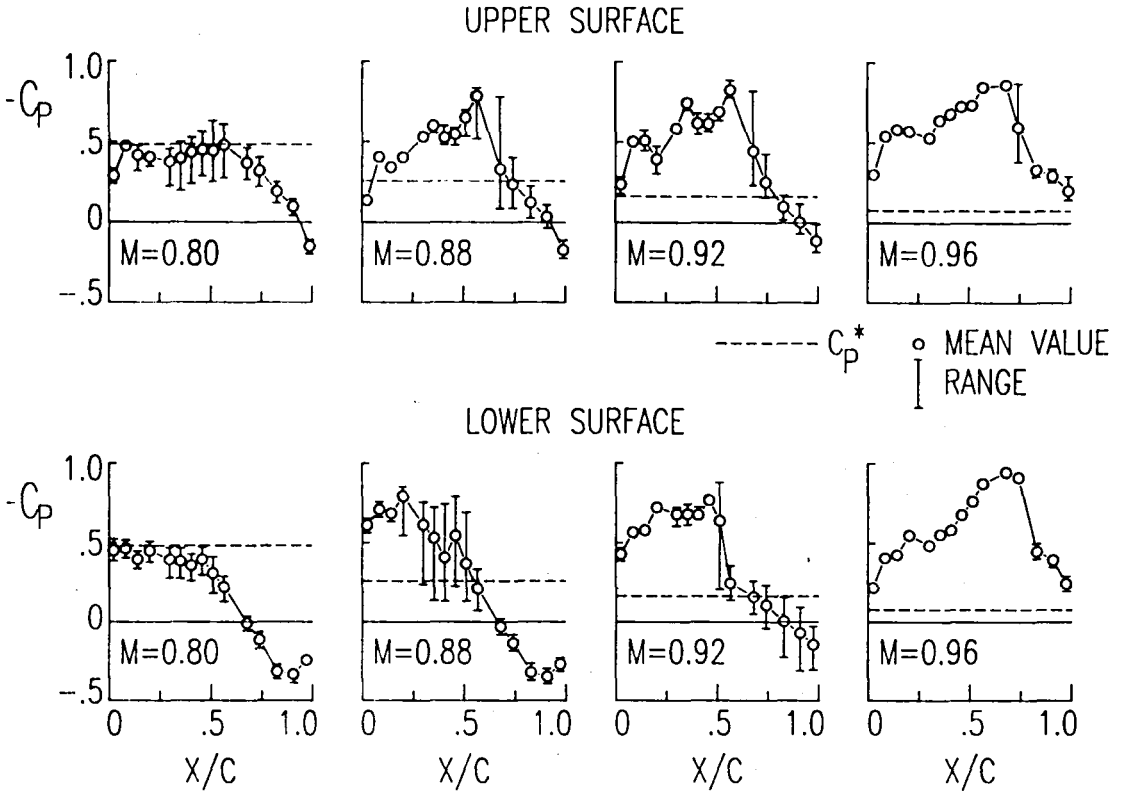

Figure 8.- Chordwise pressure distribution mean values and measurement ranges for representative Mach numbers (high q test condition, η=.87).

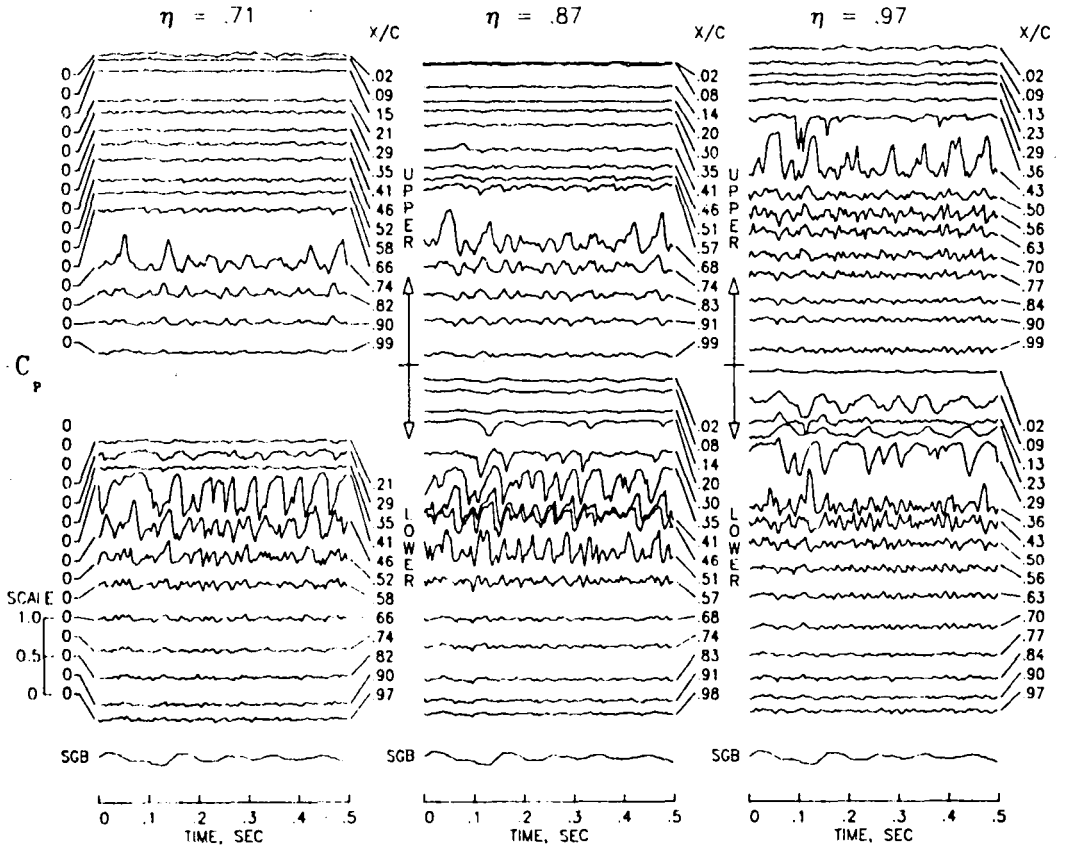

Figure 9.- Pressure time histories for M=0.88 (high q test condition).

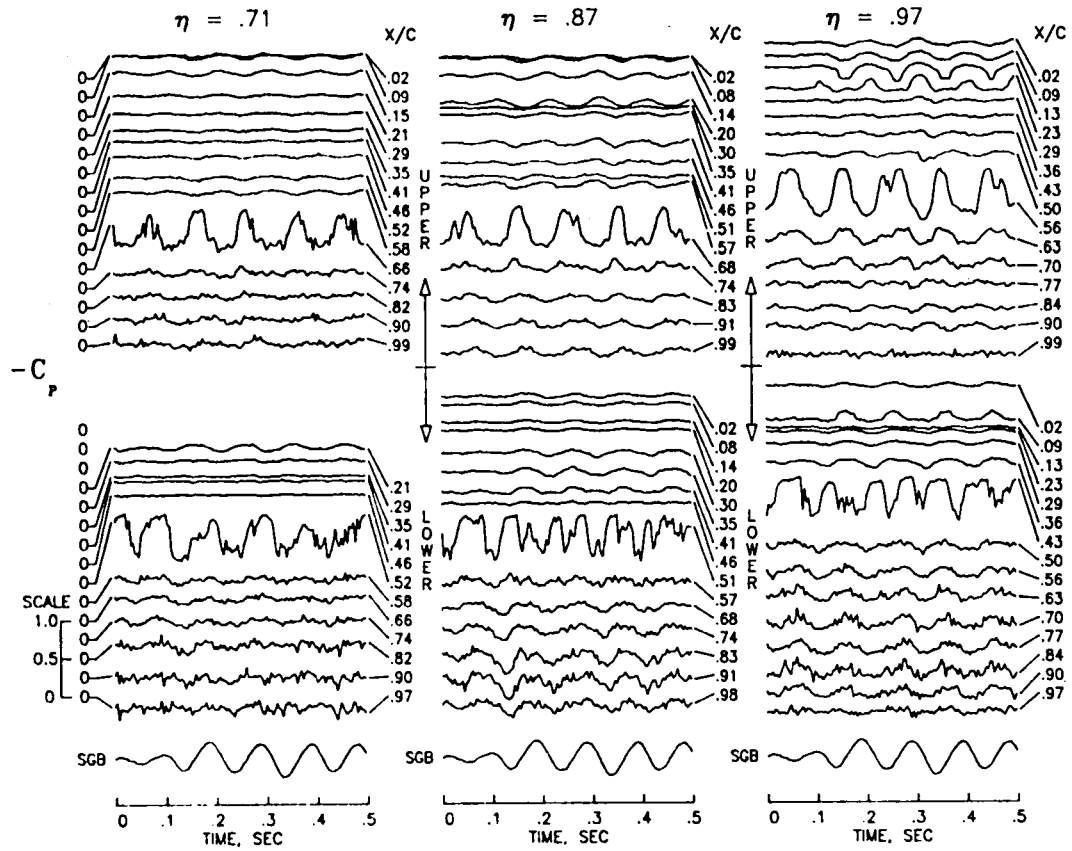

Figure 10.- Pressure time histories for M=0.92 (high q test condition).

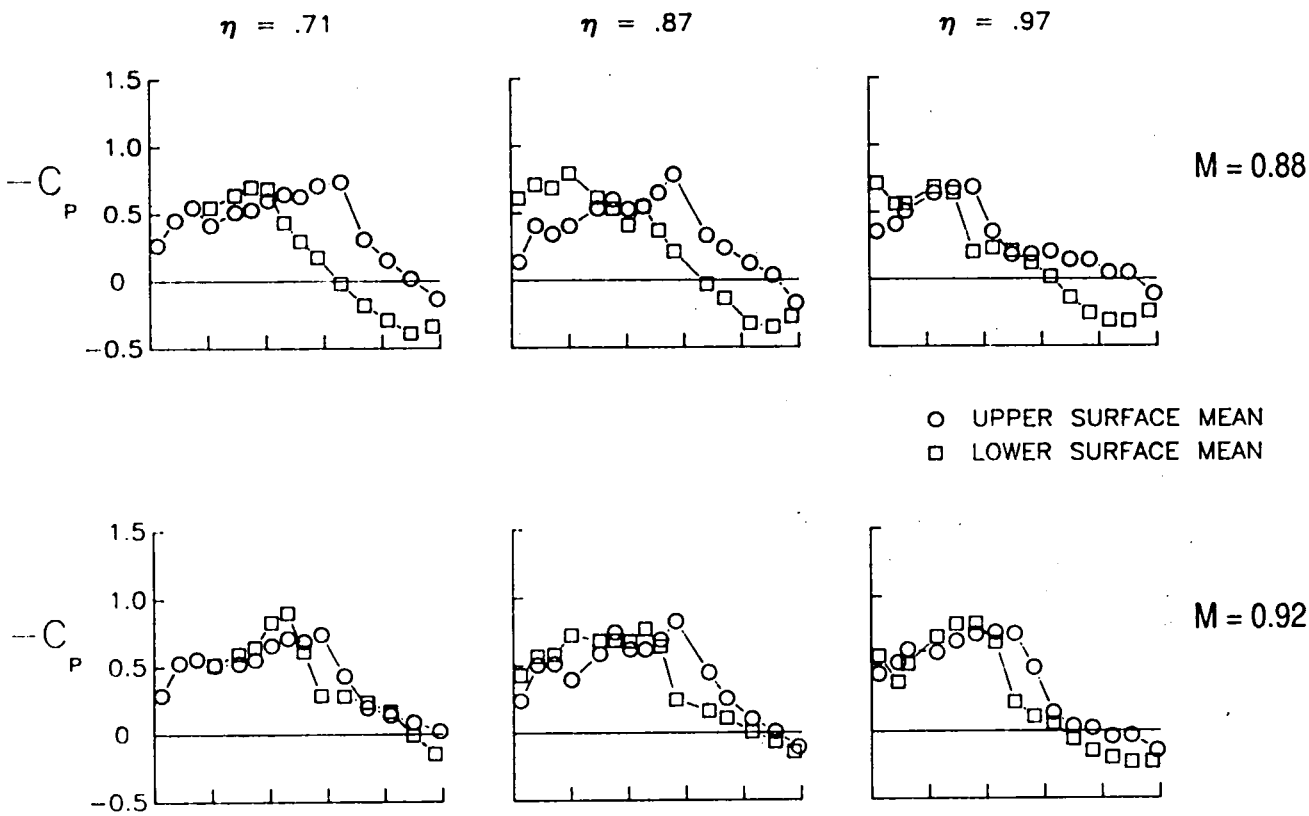

Figure 11.- Mean value chordwise pressure distributions for M=0.88 and M=0.92 (high q test conditions, three outboard orifice rows).

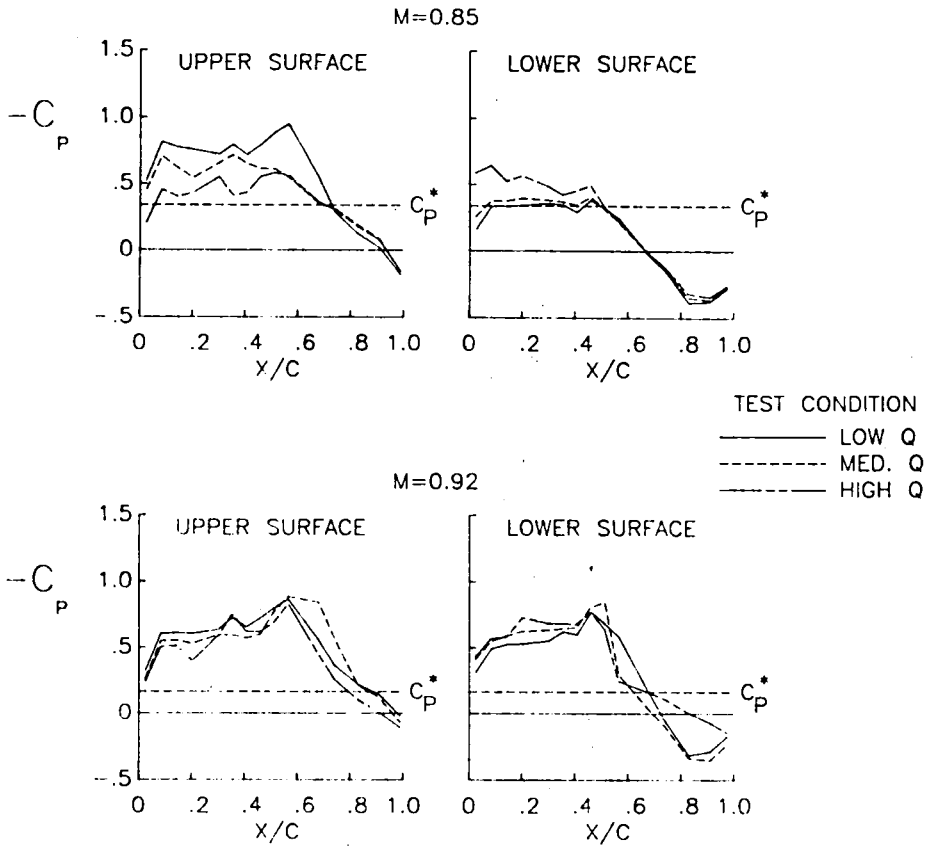

Figure 12.- Pressure distribution variations with test dynamic pressure (η=.87).

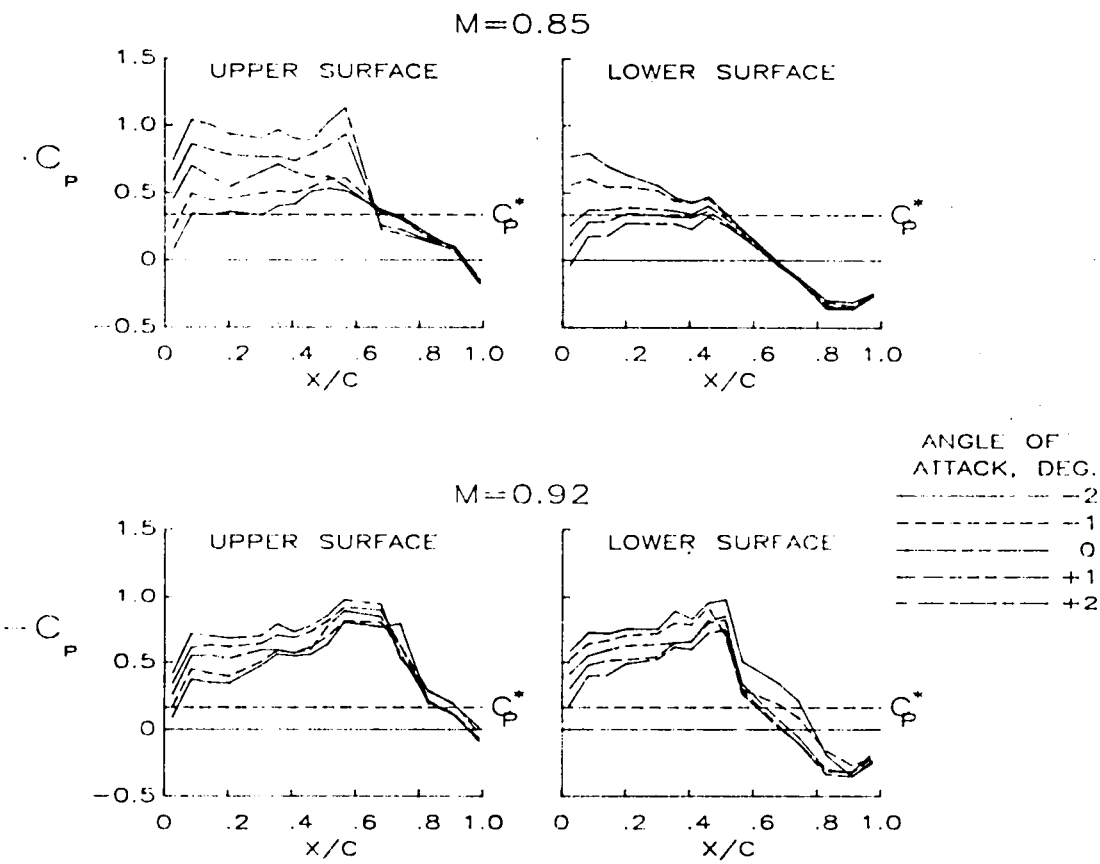

Figure 13.- Pressure distribution variations with angle of attack (medium q test condition, η=.87).

NASA National Aeronautics and Space Administration

Report Documentation Page

1. Report No.	2. Government Accession No.	3. Recipient's Catalog No.
NASA TM-100591		

4. Title and Subtitle
Unsteady Pressure and Structural Response Measurements of an Elastic Supercritical Wing

5. Report Date
May 1988

6. Performing Organization Code

7. Author(s)
Clinton V. Eckstrom
David A. Seidel
Maynard C. Sandford

8. Performing Organization Report No.

10. Work Unit No.
505-63-21-04

9. Performing Organization Name and Address
NASA Langley Research Center
Hampton, VA 23665-5225

11. Contract or Grant No.

13. Type of Report and Period Covered
Technical Memorandum

12. Sponsoring Agency Name and Address
National Aeronautics and Space Administration
Washington, DC 20546-0001

14. Sponsoring Agency Code

15. Supplementary Notes
This paper was presented at the AIAA/ASME/ASCE/AHS/ASC 29th Structures, Structural Dynamics, and Materials Conference in Williamsburg, Virginia, April 18-20, 1988, as AIAA Paper No. 88-2277.

16. Abstract
Results are presented which define unsteady flow conditions associated with high dynamic response experienced on a high aspect ratio elastic supercritical wing at transonic test conditions while being tested in the NASA Langley Transonic Dynamics Tunnel. The supercritical wing, designed for a cruise Mach number of 0.80, experienced the high dynamic response in the Mach number range from 0.90 to 0.94 with the maximum response occurring at a Mach number of approximately 0.92. At the maximum wing response condition the forcing function appears to be the oscillatory chordwise movement of strong shocks located on both the wing upper and lower surfaces in conjunction with the flow separating and reattaching in the trailing edge region.

17. Key Words (Suggested by Author(s))
Unsteady pressure
Transonic buffet
Transonic aerodynamics
Aeroelasticity
Wind-tunnel test
Supercritical wing
Aeroelasticity

18. Distribution Statement
Unclassified - Unlimited

Subject Category 02

19. Security Classif. (of this report)	20. Security Classif. (of this page)	21. No. of pages	22. Price
Unclassified	Unclassified	12	A02